Journal of
Marine Science and Engineering

MDPI

Article

Multiphase Storm Deposits Eroded from Andesite Sea Cliffs on Isla San Luis Gonzaga (Northern Gulf of California, Mexico)

Rigoberto Guardado-France [1], Markes E. Johnson [2,*], Jorge Ledesma-Vázquez [1], Miguel A. Santa Rosa-del Rio [1] and Ángel R. Herrera-Gutiérrez [1]

[1] Facultad de Ciencias Marinas, Universidad Autónoma de Baja California, Ensenada 22800, Mexico; rigoberto@uabc.edu.mx (R.G.-F.); ledesma@uabc.edu.mx (J.L.-V.); msanta@uabc.edu.mx (M.A.S.R.-d.R.); herrera.angel@uabc.edu.mx (Á.R.H.-G.)

[2] Department of Geosciences, Williams College, Williamstown, MA 01267, USA

* Correspondence: mjohnson@williams.edu; Tel.: +14-132-329

Received: 25 May 2020; Accepted: 15 July 2020; Published: 16 July 2020

Abstract: The 450-m long spit that extends westward from the northwest corner of Isla San Luis Gonzaga is one of the largest and most complex constructions of unconsolidated cobbles and boulders found anywhere in Mexico's Gulf of California. The material source derives from episodic but intense storm erosion along the island's andesitic cliff face with steep northern exposures. A well-defined marine terrace from the late Pleistocene cuts across the same corner of the island and provides a marker for the subsequent development of the spit that post-dates tectonic-eustatic adjustments. A total of 660 individual andesite clasts from seven transects across the spit were measured for analyses of change in shape and size. These data are pertinent to the application of mathematical formulas elaborated after Nott (2003) and subsequent refinements to estimate individual wave heights necessary for lift from parent sea cliffs and subsequent traction. Although the ratio of boulders to clasts diminishes from the proximal to distal end of the structure, relatively large boulders populate all transects and the average wave height required for the release of joint-bound blocks at the rocky shore amounts to 5 m. Based on the region's historical record of hurricanes, such storms tend to decrease in intensity as they migrate northward through the Gulf of California's 1100-km length. However, the size and complexity of the San Luis Gonzaga spit suggests that a multitude of extreme storm events impacted the island in the upper gulf area through the Holocene time, yielding a possible average growth rate between 7 and 8 m/century over the last 10,000 years. In anticipation of future storms, a system to track the movement of sample boulders should be emplaced on the San Luis Gonzaga spit and similar localities with major coastal boulder deposits.

Keywords: coastal boulder deposits; storm waves; hydrodynamic equations; Holocene; western North America

1. Introduction

The Gulf of California is a narrow, semi-enclosed sea that extends from its opening with the Pacific Ocean for more than 1100 km to the northwest between the Baja California peninsula and the mainland of western Mexico. As many as eight hurricanes form each year between May and October over ocean waters that attain a temperature of 27 °C or higher off the Mexican mainland near a latitude of N 15° [1]. Based on several decades of such data, 50% of such storms turn harmlessly westward into the open Pacific Ocean as they shift northward. Only a few track northeast into the Gulf of California but those that do, such as the September 2014 Hurricane Odile, are capable of causing extensive damage to infrastructure on the peninsula [2]. Odile struck the southern tip of the peninsula as a Category

4 hurricane with sustained winds reaching 215 km/h but diminished to a Category 3 event 24 h later as it tracked into the lower Gulf of California. By the time it reached the upper part of the gulf and crossed into mainland Mexico, the disturbance was reduced to a tropical storm. A detailed analysis of that storm by Gross and Mager (2020) applied mathematical models to reconstruct the impact of known meteorological conditions based on wind speed and wind direction to changes in wave height and the degree to which the water column was agitated as the storm progressed through the gulf's entire length [3]. The study's stated objective was to present a worst-case scenario on the impact of damage to tidal-energy devices that might be employed in the upper Gulf of California. Installations of this kind have yet to be built in the region, which registers tidal ranges on the order of 12 m [4]. In theory, the mechanisms engineered to harness energy from tidal exchange are not as susceptible to wind damage as they are to extreme waves. Beyond its stated purpose [3], the contribution by Gross and Mager (2020) provides the most thorough longitudinal treatment of changing physical parameters related to a major storm event in the Gulf of California.

Infrequent as they may appear on a human time frame, extreme storm events wield a measurable and persistent impact on coastal geomorphology over the long term as registered in deposits of various kinds around the world. Studies on Holocene storm chronology are focused mostly on accumulations preserved in coastal marshes, lagoons, and beach ridges [5]. Less attention has been devoted to deposits that result from the erosional retreat of sea cliffs by recurrent storm events [6–8]. On a regional basis limited to the lower Gulf of California, rocky-shore studies have focused on the Holocene development of such features where the erosion of limestone shores and volcanic sea cliffs composed of rhyolite and andesite resulted in extensive coastal boulder deposits (CBDs) and related coastal barriers [9–11]. Andesite is the most widespread rock type exposed in sea cliffs along the western Gulf of California, accounting for nearly 25% of all shoreline features including beaches and mud flats [12]. Andesite rocky coasts are under-represented compared to granite shores in the upper Gulf of California, but still common.

The goal of this study is to expand on the relationship between coastal erosion of andesite sea cliffs and the development of a massive coastal barrier deposit formed by andesite cobbles and boulders on Isla San Luis Gonzaga in the upper Gulf of California. The methods for analysis of eroded clast shapes and sizes together with estimates on the wave heights necessary for their primary generation follow those in previous contributions [9–11]. The choice of the Gonzaga study site was influenced by the prospect of superior control over the scale of sequential changes in topographic layout. It is expected that Holocene CBDs with a time range through thousands of year duration will offer better insight regarding the intensity of episodic storm events in regions like the Gulf of California otherwise perceived to suffer rare events. Civil engineers involved with planning for infrastructure ranging from artificial harbor facilities and breakwaters to potential power linkages with tidal-energy mechanisms need to be aware of such physical settings with a deep background in coastal geomorphology.

2. Geographical and Geological Setting

Located in the upper Gulf of California, the study site within Bahía San Luis Gonzaga is midway between the towns of San Felipe and Bahía de Los Angeles (Figure 1a). San Luis Gonzaga constitutes the area's largest bay (Figure 1b), covering an area of about 36 km^2. Isla San Luis Gonzaga sits at the northwest side of the bay, approximately 1.5 km^2 in area and rising 140 m above sea level (Figure 1c). Detailed geological mapping of the island and the surrounding region confirms that the local bedrock is formed entirely of andesite flows [13]. The focus of this study is a 450-m long spit formed exclusively of andesite cobbles and boulders that extends westward from the northwest corner of the island. Tracing the phased temporal development of the spit ranks as the project's primary goal, which entails advantages in scale and layout compared to earlier studies of CBDs in the lower Gulf of California [9–11].

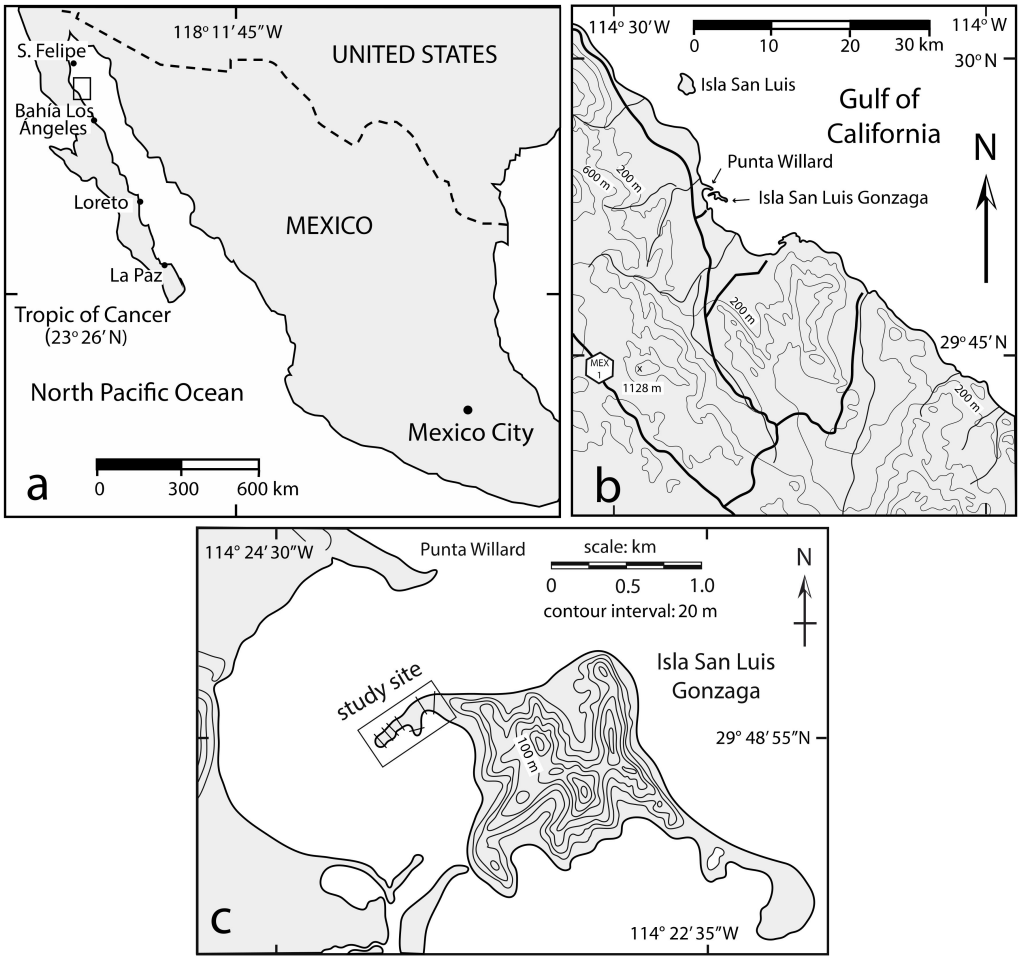

Figure 1. Locality maps showing Mexico's Baja California peninsula and Gulf of California; (**a**) Mexico and border area with the United States denoting key towns with inset box marking the study area between San Felipe and Bahía de Los Angeles; (**b**) Region around Bahía San Luis Gonzaga showing Isla San Luis Gonzaga in the northwest part of the bay; (**c**) Topographic map of Isla San Luis Gonzaga with the study site marked (box) within which the study transects are indicated.

3. Materials and Methods

3.1. Data Collection

Isla San Luis Gonzaga was visited in June 2019, when the original data for this study were collected from unconsolidated andesite clasts forming the long spit attached to the island accessible from Punta Willard (Figure 1c). Cobble- and boulder-size clasts encountered on tape lines through seven transects were measured manually in three dimensions perpendicular to one another in each clast (long, intermediate, and short). All transects were laid out to cross the spit at different locations, always at right angles to the defining shore with orientations recorded by compass. Continuous tracking of elevation with respect to sea level was monitored across each transect in order to construct topographic relief profiles (see Section 3.2 for more details). Differentiated from cobbles, the base definition for a boulder adapted in this exercise is that of Wentworth (1922) for an erosional clast equal or greater than 256 mm in diameter [14]. No upper limit for this category is defined in the geological literature. Triangular plots were employed to show variations in clast shape, following the design of Sneed and Folk (1958) for river pebbles [15]. Comparative data on maximum cobble and boulder dimensions were fitted to bar graphs to show variations in composition from one transect to the next. Multiple samples

of andesite were collected from the island's rocky-shore zone for laboratory analysis to determine specific gravity.

3.2. Aerial Photography and Applications for Topography

Use of a DJI Inspire 2 Drone™ (DJI, Nanshan District, Shenzhen, China) was employed to generate the Geographic Information System (GIS) platform, photogrammetry, and digital elevation model (DEM) in this study following standard protocols [16]. Eight tarps, each covering 1 m^2, were printed with a highly visible pattern that could clearly be detected from the sky. The tarps were laid out across the rocky bar and georeferenced using a handheld Geographic Positioning System (GPS). Thereafter, a flight plan was designed and uploaded to the drone with a limited flight duration between 23 and 27 min that was ample for completion while providing a stable platform. The flight plan was designed to calculate the number of images the drone needed to take based on altitude and desired image overlay (70–80%). Each image captured by the drone was automatically georeferenced and transferred to photogrammetry software, where steps were followed to join the images into a single mosaic. The first step is image alignment, wherein the software places and aligns the images taken by the drone based on the GPS data from the flight plan, as well as the control points from the tarps and GPS data collected on sight. The next step entailed object identification so that tie points could be generated to stitch the images together. A sparse cloud was next generated from a series of points using the overlaid images, points in common, and drone flight data to calculate the elevation of each point. With these data from the dense cloud, a mesh is created as a series of triangles that joins the points from the dense cloud, and the resulting layer is a continuous surface on which the original images can be "draped over". Based on the generated data in the previous step, a DEM can be generated using the kriging interpolation method. For example, the same strategy has a successful application for high accuracy surveying of beach-sand topography [17].

Using GIS software by Agisoft Metashape, the DEM was applied to determine the slope and direction of the slope traversing the spit. To determine slope the software calculates the angle on the incline based on the elevation of each pixel and its relation to the adjoining pixels. With the slope layer generated and geographic location of the layer the software determines the downslope direction for each cell within the DEM. The resulting layer indicates the main slope directions of the feature. To obtain the elevation of the associated marine terrace, its location was georeferenced from images taken by the drone. A digital marker was placed on the edge of the marine terrace. This marker was used as a geo-reference in the DEM and the elevation data were extracted with the aid of an "Identify tool." The same methodology was used to extract the height data of the highest point of the adjoining spit.

3.3. Hydraulic Model

With determination of specific gravity based on the value of 2.3 g/cm^3 for andesite, a hydraulic model may be applied to predict the energy needed for the erosion of joint-bound blocks from a rocky shoreline and their subsequent transfer to an adjacent coastal boulder deposit as a function of wave impact. Andesite is a volcanic rock that forms from surface flows with variable thicknesses and a propensity to develop vertical fractures. These factors regulate the size and general shape of blocks loosened by erosion in the cliff face. Herein, two formulas are applied to estimate the magnitude of storm waves against joint-bounded boulders derived, respectively, from Equation (36) in the original work of Nott [18] (Equation (1)) and from an alternative formula that uses the velocity equations of Nandasena et al. [19] as applied by Pepe et al. (2018) [20] to estimate wave heights (Equation (2)):

$$H_S = \left(\frac{\left(\frac{\rho_s - \rho_w}{\rho_w}\right) a}{C_l} \right) \quad (1)$$

$$Hs = \frac{\frac{2\left(\frac{\rho s - \rho w}{\rho w}\right).\ c\ .\ [\cos F + (\mu_s\ .\ sin\ F)]}{c_1}}{100} \quad (2)$$

where H_s is the maximum height of the storm wave at breaking point; ρ_s is the density of the boulder (2.3 g/cm^3); ρ_w is the density of water at 1.02 g/cm^3; a is the length of boulder on long axis in cm; c is the length of boulder on short axis in cm; θ is the angle of the bed slope at the pre-transport location (1° for joint-bounded boulders); μ_s is the coefficient of static friction (= 0.7); and C_l is the lift coefficient (= 0.178). Equation (1) is more sensitive to the length of a boulder at the long axis, whereas Equation (2) is more sensitive to the length of a boulder on the short axis. Therefore, some differences are expected in the estimates of H_S.

4. Results

4.1. Base Maps and Transect Lines

A set of base maps constructed on the basis of aerial photography illustrate the principal attributes of the spit (Figure 2), as located on the topographic map in Figure 1c. The massive agglomeration of loose cobbles and boulders extends for a distance of 450 m westward from the source at sea cliffs on the north side of Isla San Luis Gonzaga. A mosaic image pieced together from the aerial survey and shown in natural sunlight (Figure 2a), marks the location of seven transects with the first (T1) closest to the source of eroded andesite clasts on the north face of the island and the last (T7) most distal at the end of the spit. The surface area represented by the spit amounts to 15,600 m^2, of which less than 5% is obscured by plant cover dominated by the Sweet Mangrove (*Maytenus phyllanthoides*) [21]. Variations in topography (Figure 2b) reveal that the maximum elevation through the central axis of the spit rises to 3 m above mean sea level. Variations in slope direction along the divergent axes of the spit descend dominantly to the northwest (Figure 2c). Key aspects related to the layout of all transects and registered content are compiled in Table 1.

Table 1. Comparative data drawn from transect lines across the bar system at Bahía San Luis Gonzaga.

Transect	Length (m)	Compass Orientation	Total Clasts Measured	Cobbles (%)	Boulders (%)	Clast Density (Clast/m)
1	37	181.15°	95	36	64	2.6
2	33	147.22°	85	36	64	2.6
3	24	60.77°	77	92	8	3.2
4	25	147.29°	56	45	55	2.2
5	28	143.58°	125	77	23	4.5
6	28	146.31°	110	75	25	4.4
7	30	122.66°	112	51	49	3.7
Mean	29	135.55°	94	59	41	3.3

Average transect length amounts to 29 m and the dispositions of all but transect 3 are roughly parallel, oriented along a NW to SE trend. Transect 3 follows an orientation roughly 90° out of phase with the others, trending NE to SW. The average density of cobble and boulder clasts measured per transect is substantial at 94 with an average spacing of 3.3 clasts per meter. Transect 3 records the fewest boulders compared to all other transects at less than one in 10. Overall, the dominance of boulders over cobbles is greatest in transects 1 and 2 located most proximal to the source rocks at the beginning of the spit at a ratio 2:1. That ratio falls closer to parity between cobbles and boulders in transect 4 diagonal to the spit roughly midway along its length. Farther out along the spit in transects 5 and 6, the ratio of boulders to cobbles is 1:3. Near the tip of the spit (Figure 2a), transect 7 is the most distal from the source of eroded clasts and reflects a modest return in the relationship between boulders and cobbles at parity.

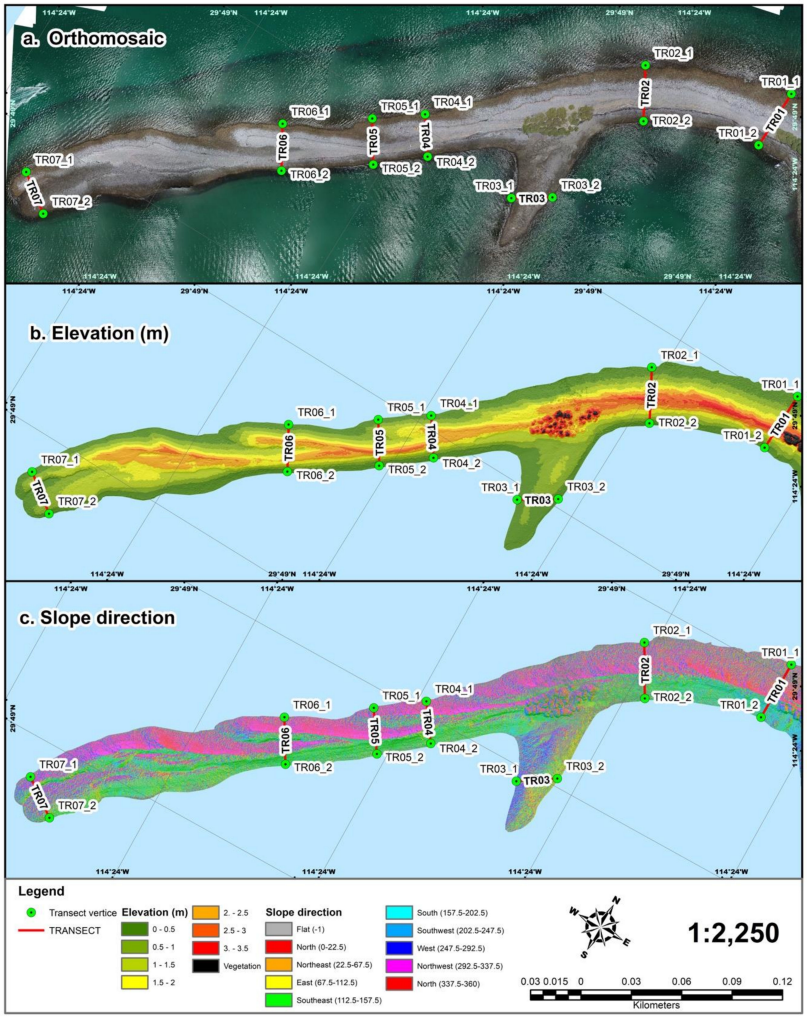

Figure 2. Base maps for the unconsolidated spit off the northeast end of Isla San Luis Gonzaga; (**a**) Orthophoto mosaic under natural light showing the position of transects 1 to 7; (**b**) Orthophoto color-coded map showing variations in elevation above mean sea level; (**c**) Color-coded map showing variations in slope direction.

4.2. Source of Joint-bound Blocks

Equations (1) and (2) from Nott (2007) and Pepe et al. (2018) [18,20] are specific to wave energy applied at the source against joint-bound blocks exposed in rocky shorelines. All materials subsequently transferred to the 450 m long spit at San Luis Gonzaga originated due to wave erosion against andesite cliffs exposed on the north side of the island. The rocky shore extends EW for almost a kilometer, rising topographically to 60 m, or more (Figure 1c). Sea cliffs in the area nearest the spit exhibit andesite flows with bedding planes that dip at a high angle to the west with irregular joints perpendicular to bedding planes (Figure 3a,b). Large blocks of andesite only crudely rounded by abrasion occupy the intertidal zone on a wave-cut platform at the side of an uplifted marine terrace. Fresh material in the supratidal zone lacks the darker tone of blocks colored by organic growth.

4.3. Andesite Specific Gravity

Five samples of andesite from the north shore of Isla San Luis Gonzaga yielded a range of values for specific gravity between 2.26 and 2.34 gr/cm^3. The samples ranged in weight between 215 and 620 gm and were displaced between 151 and 271 mL of water. The mean value calculated from

the samples amounts to 2.3 gr/cm^3 and this value was uniformly applied to Equations (1) and (2) in estimation of wave heights provided in Tables A1–A7.

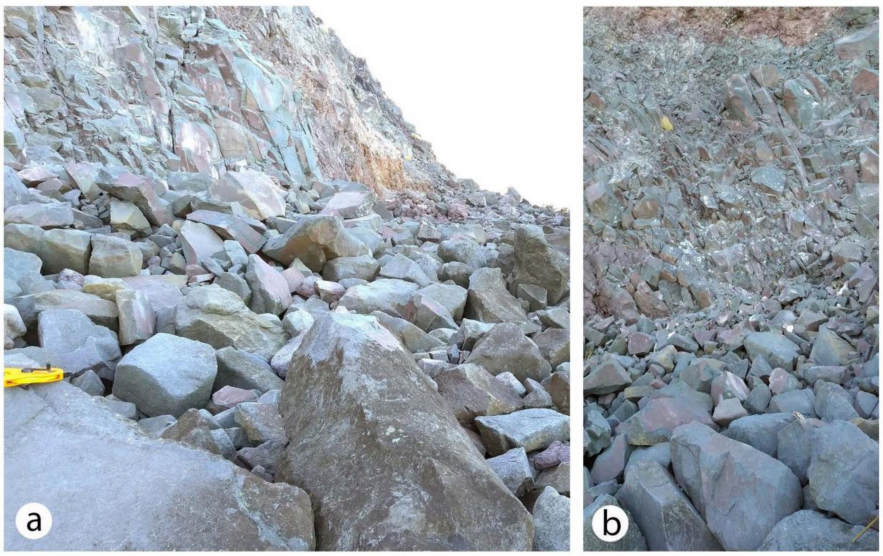

Figure 3. Rocky shore and intertidal zone at cliffs adjacent to the marine terrace and near the start of the 450-m long spit on Isla San Luis Gonzaga; (**a**) Oblique view with housing of meter tape for scale; (**b**) Head-on view showing tilted andesite flows in the background.

4.4. Comparative Variation in Clast Shapes

Raw data on boulder size in three dimensions collected from each of the seven transects are available in Appendix A (Tables A1–A7). Due to the wealth of data collected in the field, the size of Tables A1 and A2 is limited to a representative sample based on 50% of the boulders. Table A3 is the smallest, because few boulders were encountered, all of which are included. Likewise, all boulders from transects 4 to 7 are enumerated in Tables A4–A7. With regard to shape, points representing individual clasts (including smaller cobbles) are shown grouped by transect and plotted on a set of Sneed–Folk triangular diagrams (Figure 4a–g). The spread of points across all seven of the plots is remarkably consistent, showing a strong similarity in the variation of shapes from one transect to another. It is seldom that points fall into the upper-most triangle, which represents an origin from a cube-shaped endpoint. The majority of points from all seven plots falls within the middle part of the two tiers below the top triangle. Those points clustered at the core of any given triangular plot are representative of clasts for which two dimensions are closer in value than the third measured along the shortest axis. However, a significant portion of points falls into the middle-right and lower-right domains of the field, which signifies a tendency for development of elongated shapes eroded from bar-shaped blocks of source rock. The composite slope of points across all plots from the few in the topmost triangle to those in the lower right corner of the field demonstrates a tendency for development of moderately oblong shapes. Rarity of points in the middle bottom tier and complete absence of points in the lower-left corner of triangular plots indicates that the wave-eroded material from the parent sea cliffs excludes plate-shaped blocks.

4.5. Comparative Variation in Clast Size

Clast size is conveniently plotted on bar graphs as a function of maximum length based on the original data (see Tables A1–A7 for boulders). Transect 1 (Figure 5) is the station physically closest to the bedrock source and, in principal, is expected to reflect the highest proportion of boulders.

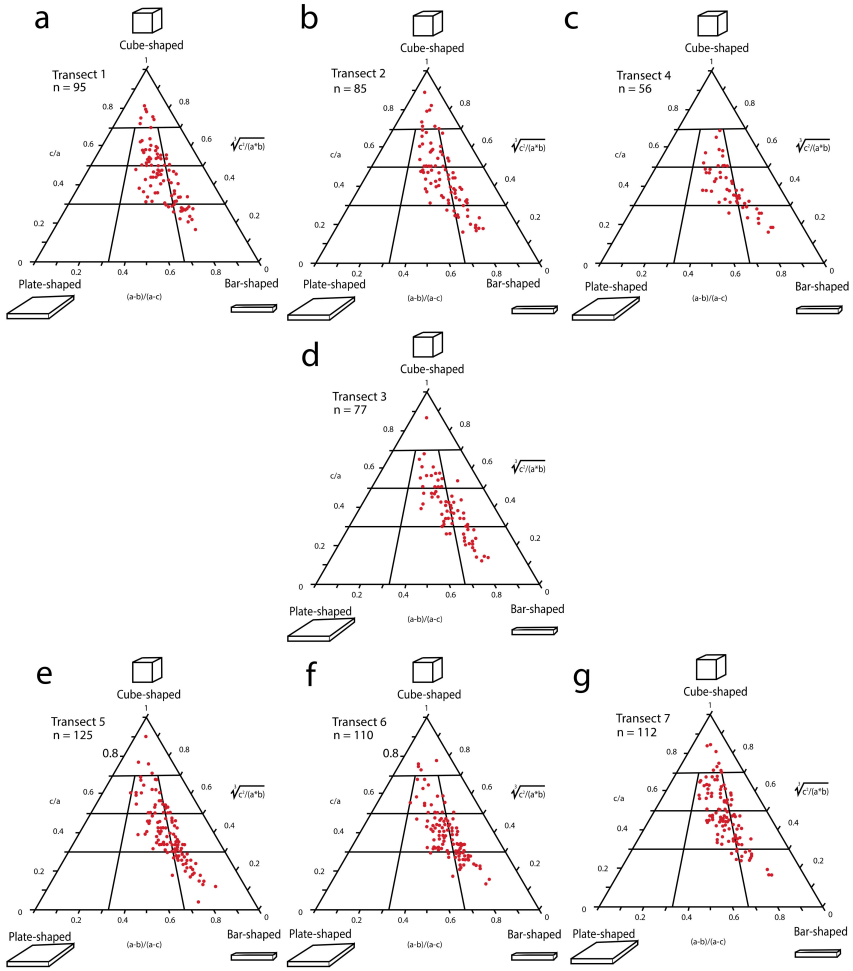

Figure 4. Set of triangular Sneed–Folk diagrams used to appraise variations in cobble and boulder shapes; (**a**) Trend from transect 1 closest to sea cliffs at the source of the clasts; (**b**) Trend from transect 2; (**c**) Trend from transect 4; (**d**) Isolated trend from transect 3 with a markedly different orientation from all other transects; (**e**) Trend from transect 5; (**f**) Trend from transect 6; (**g**) Trend from transect 7 most distant from sea cliffs at the common source of all clasts in the system.

Conversely, transect 7 is most distal from the bedrock source and is expected to show a higher proportion of cobbles. Groupings separated in bins at intervals of 5 cm are arrayed in histograms stacked to show differences in size range between 6 cm and 90 cm among transects 1, 2, and 4 (Figure 6a–c). Data for transect 1 (Figure 6a) registers the highest concentration of small boulders. Transect 3 projects as a side spur on the southeast side of the spit (Figure 7). It is excluded from this analysis due to the relative scarcity of boulders. Each of the three graphs in Figure 6 delineates the boundary between cobbles and boulders with a dashed line. They are consistently skewed with the highest percentage of clasts at or around the border between the largest cobbles and smallest boulders. The ratio between boulders and cobbles remains steady at 2:1 in transects 1 and 2 but is closer to parity in transect 4. Compared to the proximal transects, the more distal transects 5 to 7 (Figure 8a–c) exhibit a marked shift in skewness to a numerical domination by cobbles. In transects 5 and 6, the relationship between boulders to cobbles is roughly consistent dropping to a ratio of 1:3. However, data from transect 8 at the distal end of the spit (Figure 8c) records a ratio at parity. In all cases among the six transects represented by bar graphs, the extreme outlier of large boulders occurs at measured lengths between 76 cm and 85 cm.

Figure 5. Transect 1 (dashed line) features the highest concentration of small and intermediate size boulders. The survey line passes through the spit about 40 m beyond the marine terrace at the NE corner of Isla San Luis Gonzaga. Superposition of white arrows defines the outer lip of the marine terrace elevated 8.5 m above sea level.

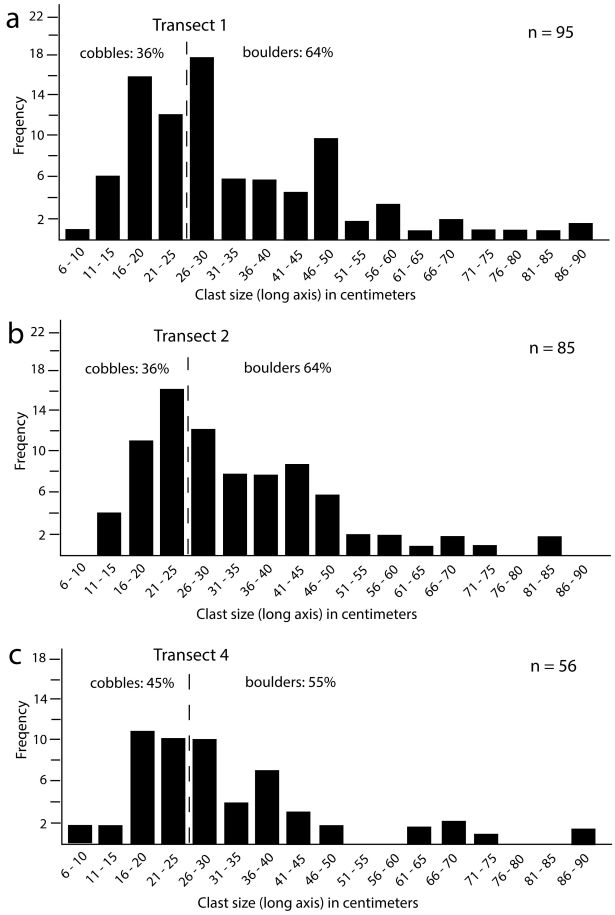

Figure 6. Set of bar graphs used to appraise variations in maximum boulder length from the three transects with similar orientations closest to the source of coastal erosion; (**a**) Bar graphs from transect 1; (**b**) Bar graphs from transect 2; (**c**) Bar graphs from transect 4. Transect 3 is excluded from this treatment on account of its deviant orientation.

Figure 7. Transect 3 (dashed line) follows a side spur off the main spit with a compass orientation 90° out of phase with other transects. Boulders are uncommon, but the largest in the foreground exceeds 50 cm in diameter. The spur is notably isolated from the opposite side of the spit by a dense thicket of Sweet Mangrove (*Maytenus phyllanthoides*) and is largely submerged during high tide.

4.6. Variation in Transect Profile Elevations

Data recovered from the seven transects in this study (Figure 2) also include the requisite information for construction of individual elevation profiles. The highest elevation determined at the crest of any single transect amounts to no more than 3 m above mean sea level. Transects 1 to 3 were found to conform to profiles that rise evenly to peak elevation at or near the center of the transect from opposite ends and are not illustrated. In contrast, transects 4 to 6 (Figure 9) exhibit profiles with a marked depression at variable positions along the line. Transect 4 (Figure 9a) registers a modest decline in elevation of 50 cm across the central 5 m of the line. Transect 5 (Figure 9b) shows a similar dip but is skewed much closer to the NW end of the transect. Transect 6 (Figure 9c) exhibits the deepest depression midway through the line with a drop of about a meter. Transect 7 also features a bifurcated elevation profile, but it is not shown at the same scale because it represents a much lower overall value in maximum elevation at only 1.2 m. Among the seven transects, transect 3 (see Figure 7) registered the lowest elevation rising to only a half meter above sea level.

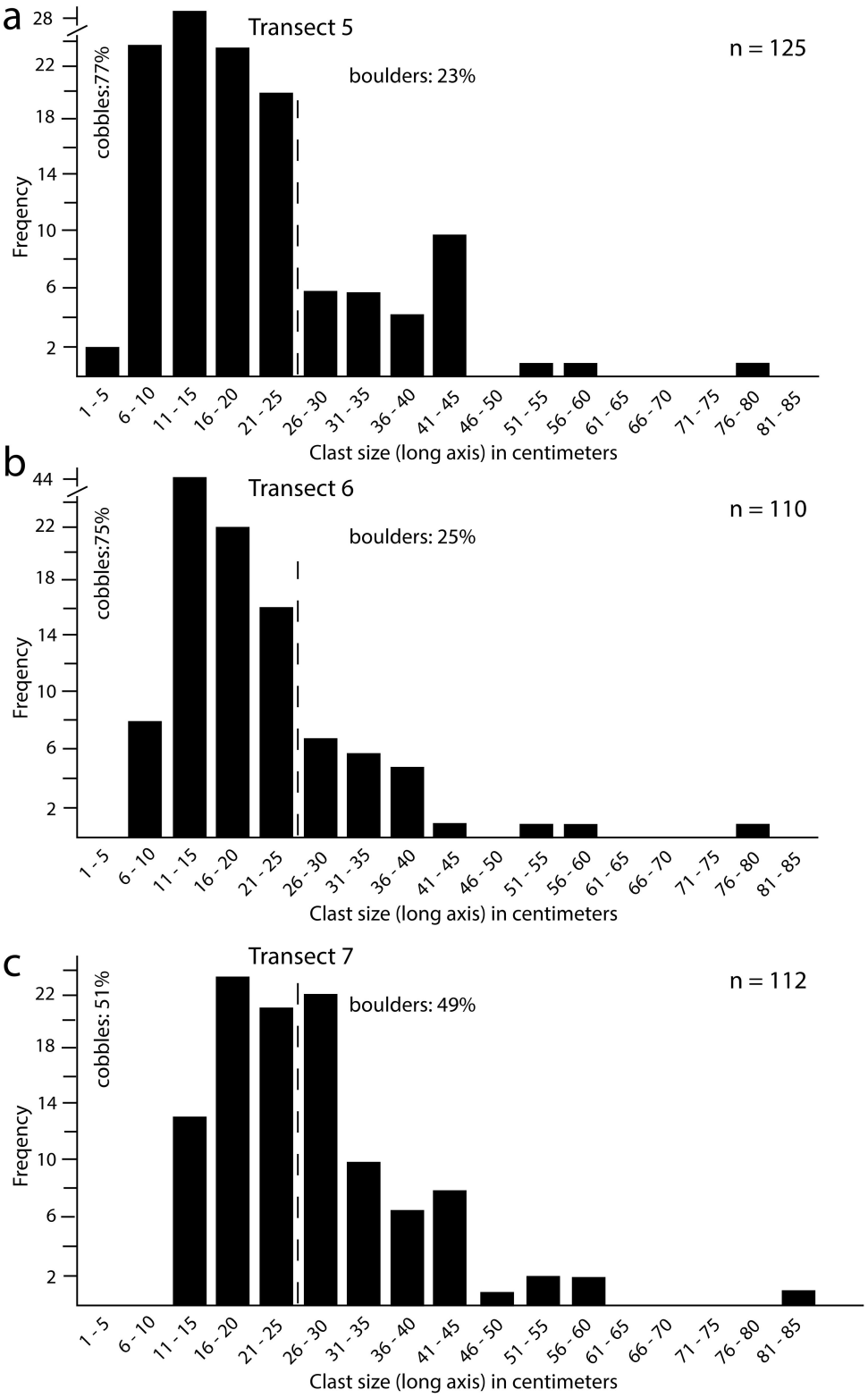

Figure 8. Set of bar graphs used to appraise variations in maximum boulder length from the three transects with similar orientations most distal from the source of coastal erosion; (**a**) Bar graphs from transect 5; (**b**) Bar graphs from transect 6; (**c**) Bar graphs from transect 7.

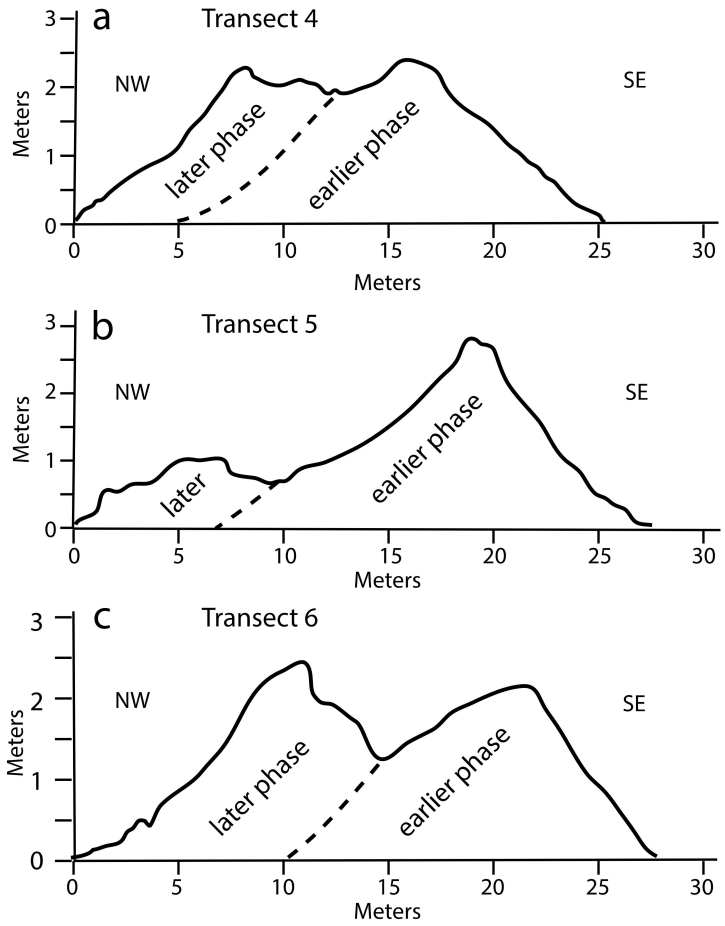

Figure 9. Comparison of selected transverse profiles in the distal part of the spit showing separation of different phases in the overall deposit. Transects 1–3 and 7 lack such distinct features; (**a**) Elevation profile through transect 4; (**b**) Elevation profile through transect 5; (**c**) Elevation profile through transect 6. See Section 3 for source of the elevation data.

The long view over the spit's axis to the NE from a location on transect 4 (Figure 10) captures the nature of the depression cutting diagonally through the more proximal part of the structure. Thus, the transverse depression in transect 4 is defined by a pair of longitudinal bars that distinctly separate one side of the spit from the other with an intermediate trough. From this vantage, it may be realized that the spit underwent a growth history in sequential phases. Following from this insight, the ramification is that the Sneed–Folk plots in Figure 4c,e,f, as well as the bar graphs in Figures 6c and 7 represent consecutive phases of development that occurred over time. In contrast, the elevation profiles for transects 1–3 that conform to a simple arc in relief, imply that the Sneed–Folk plots and bar graphs relevant to those transect samples reflect more unitary slices temporal development.

4.7. Biological Data from Encrusted Boulders

From place to place, disarticulated bivalve shells (including *Anadara grandis* and *Megapitaria squalida*) appear sporadically among the mixed cobbles and boulders forming the spit. The degree of breakage in some of the larger shells indicates a higher level of energy was entailed in their delivery to the spit, more than from normal conditions related to tidal flux. More significant are examples of large boulders encrusted by the common oyster (*Ostrea palmula*) that thrives in intertidal waters throughout the Gulf of California [22]. A block with a long axis of 70 cm found near transect 7 hosted more than two dozen oysters on its upper surface (Figure 11a) before it was transported onto the spit and left upside down. In contrast to the inarticulate shells found elsewhere separately as disarticulated shells,

the oysters are encrusted in growth position and many remain articulated (Figure 11b). The biological inference is that the boulder originally sat submerged in the shallow water off to the side of the spit and was subsequently carried onto the spit by a storm of sufficient strength to lift an andesite block weighting as much as 80 to 100 kg (see range of weights in Table A7). The pristine condition of the oyster shells suggests that the storm was a relatively recent event. Weaker storms are capable of transporting cobles and smaller boulders during earlier events and may have shifted the offshore position of the block until the next major storm moved it onto the spit.

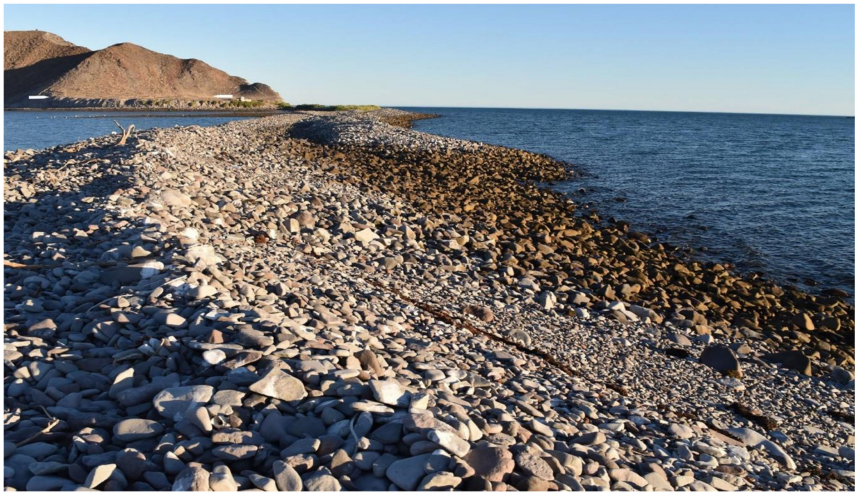

Figure 10. View across transect 4 northeast toward the connection with Isla San Luis Gonzaga, showing a distinct swale between two different phases of the cobble-boulder deposit. Note the raised Pleistocene marine terrace in the far distance (white arrows). The inner wall of the marine terrace is oriented NS.

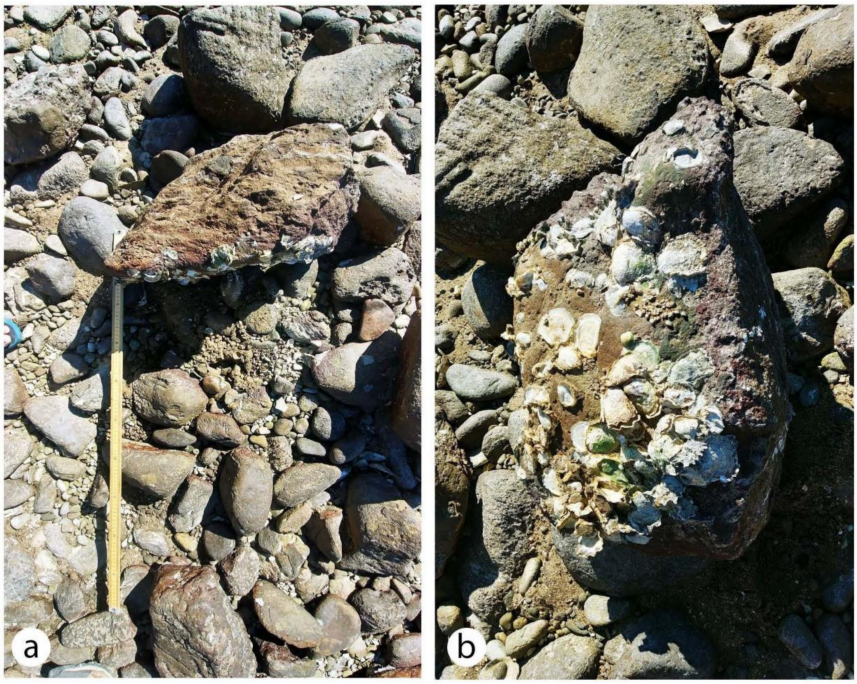

Figure 11. Contemporary oysters (*Ostrea palmula*) encrusted on a boulder near transect 7; (**a**) Boulder as first encountered on the spit (meter stick for scale); (**b**) Same boulder overturned for better view of encrusting oysters, approximately 7 cm in shell length. Note: many of the oysters remain articulated.

4.8. Storm Intensity as Function of Estimated Wave Height

Average boulder sizes and maximum boulder sizes from all seven transects are summarized in Table 2, whether or not the respective Sneed–Folk diagrams and bar graphs (Figure 4, Figure 6, and Figure 8) reflect solitary events or an agglomeration of phased events. These data are a prerequisite for comparison of results estimating wave heights first directed against joint-bound blocks on the andesite rocky shore as derived from the Nott formula [18] and the subsequent formula applied by Pepe et al. [20]. There exists a general trend in reduction of average boulder size from transect 1 to transect 5 more than halfway along the Gonzaga spit from the proximal source. Thereafter in transects 6 and 7, there occurs an increase in average boulder size. The estimated mean wave height necessary to transport those boulders extracted from the rocky shore amounts to 2.7 m according to the Nott formula. However, at 73 cm the mean maximum boulder length derived from all seven transects yields a value almost twice the diameter for the average of all averages (Table 2). Moreover, the estimated mean weight of the largest single boulder from each transect amounts to 200 kg, which is more than 4.5 times the average weight computed from all boulders surveyed in the seven transects. The estimated wave height needed to shift the largest boulder in transect 7 amounts to nearly 6 m according to the Nott equation, but half that compared with the Pepe equation. However, results based on the Pepe equation for the largest boulders yield a higher wave height in four out of seven transects. In general agreement with the biological inference from the oyster-encrusted block in Figure 11, the critical insight from these comparative data is that the average impact from smaller waves is sufficient to move smaller boulders, but only the largest waves are sufficient to move the largest boulders.

Table 2. Summary data from Appendix A (Tables A1–A7) showing maximum bolder size and estimated weight compared to the average values for sampled boulders from each of the transects together with calculated values for wave heights estimated as necessary for CBD mobility. EWH = estimated wave height.

Transect	Number of Samples	Mean Boulder Size (cm^3)	Mean Boulder Weight (kg)	Estimated Mean Wave ht. Nott [18] (m)	Max. Boulder Size (cm^3)	Max. Boulder Weight (kg)	Max. EWH Nott [18] (m)	Max. EWH Pepe et al. [20] (m)
1	32	43.5	81	3.0	90	628	6.3	7.6
2	33	40	59	2.8	64	139	3.7	5.6
3	6	36	12.75	2.7	61	35	4.3	1.3
4	32	40	36	2.8	75	191	5.3	5.6
5	29	25	29.5	2.6	57	166	4.0	6.1
6	20	35	25	2.4	80	190	5.6	3.7
7	30	38	47	2.6	84	122	5.9	3.2
Mean	26	37	43	2.7	73	200	5.0	4.7

5. Discussion

5.1. Phased Development During Holocene Time

As projected by the orthophoto mosaic in Figure 2a and supplemented by transect elevation profiles derived from seven transects, the overall layout of the unconsolidated cobble-boulder spit at Isla San Luis Gonzaga suggests an interpretation of growth through multiple phases during Holocene time. A starting point in post-Pleistocene time is supported by the physical connection of the spit to the island adjacent to an uplifted marine terrace (see photo in Figure 5). The terrace truncates the northwest corner of the island and its outer lip rises 8.5 m above the base level of the spit. Marine erosion on the terrace ceased prior to initiation of the spit around the present sea level. The recessed terrace flat is relatively clean, showing that the Pleistocene sea cliff at the rear of the terrace was not the parent source of eroded clasts contributing to the spit. Instead, the yet active source appears along the modern sea cliffs that stretch across the northern part of the island. At the proximal end of the spit, sea cliffs on the north exposure rise steeply up to 60 m in height (Figure 1c). Headward erosion of a modern wave-cut platform cuts into the base of adjoining sea cliffs that provide the copious raw materials derived from joint-bound blocks (Figure 3). Large blocks are first smoothed by wear in the surf and subsequently

transferred by storm currents in a SW direction to the spit. Undermining of the sea cliff by storm action also contributes to rock falls from higher in the exposure.

Creation of the 450-m long spit is interpreted as having evolved over the last 10,000 years during a succession of episodic storm events outlined in Figure 11. Progradation of the spit at the outset between transects 1 and 2 follows a linear pattern that left a consistent profile tracing a single, central rise in elevation roughly midway between side margins (Figure 2b). The next phase of construction entailed a curvature to the south that terminated beyond the position of transect 3 (Figure 12a). The profile across transect 3 reflects a low median rise in elevation (see Figure 7). A dense thicket of vegetation north of transect 3 (Figure 2a) signals this phase of development terminated as a side spur that ceased to receive fresh material and became isolated from the rest of the structure. Resumption of deposition with a linear extension to the SW pushed a narrow lobe of the spit beyond transect 4 (Figure 12c), presumably due to a change in storm dynamics. The pair of topographic bars that form parallel swales in transects 4 and 5 (Figure 9a,b) mark the further expansion of the spit to the SW with the more easterly bar deposited during an earlier storm event and the adjoining bar amalgamated alongside during a later event. Physical compression of the two storm events resulted in expansion of the spit's width across transects 4 and 5.

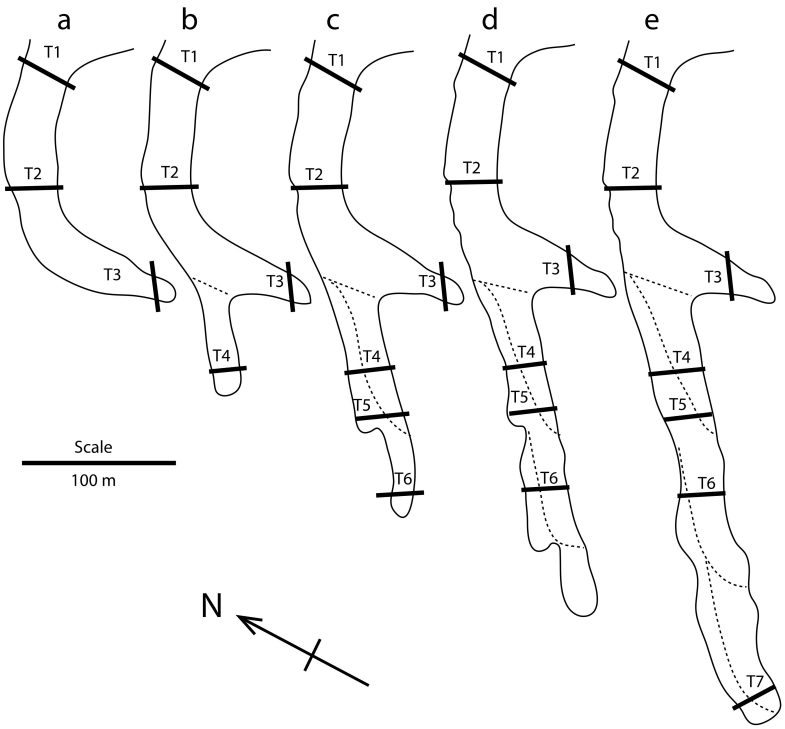

Figure 12. Interpretation of temporal development through Holocene time with study transects marked as reference points: (**a**) phase one; (**b**) phase two; (**c**) phase three; (**d**) phase four; (**e**) phase five. Dashed lines mark boundaries between successive additions to the structure through time.

A similar sequence of staggered events took place with further extension of the spit to the SW beyond transect 6 (Figure 12d). During the earlier phase of expansion in this area, the spit was narrower but doubled in width with amalgamation of the adjoining later phase. The pattern repeated itself, once again, under progradation of the spit beyond transect 7 (Figure 12e) to reach the present terminal length of 450 m. The number of discrete storm events that contributed to the phased growth of the spit is difficult to estimate, but the presence of boulders across all transects makes clear that major storms were involved.

The incremental rate of the structure's progradation from the bedrock source on Isla San Luis Gonzaga is difficult to calculate with any accuracy, but an estimate can be offered on the assumption

that phased growth resulted from storms of hurricane strength that occurred as often as every 100 years. This metric is suggested in reference to the popular notion of recurrent events outside the living memory of a long human lifetime. Holocene mega-storms with a measurable recurrence between 100 and 300 years are tested on the basis of coastal storm ridges that incorporate coral heads dated by isotope chronology [5]. Recurrence of mega-storms on a centennial scale also is suggested by the isotope chronology of speleothem deposits from caves commonly impacted by landfall of tropical cyclones [23]. No such method of absolute dating is possible with regard to the storm-deposited andesite boulders from Isla San Luis Gonzaga. The rocks are dated by radiometric means, but the dates so derived represent the age when lava flows solidified during the Miocene [13] and not the time of coastal erosion.

Storms of hurricane intensity reaching Isla San Luis Gonzaga would have entailed wave heights at or exceeding 5 m based on equations from Nott [18] and Pepe et al. [20]. Such waves would impact the island's north shore following a pattern of cyclonic rotation with northward travel. Extraction of large andesite blocks from the base of the sea cliffs (Figure 3) was influenced by hydraulic wedging of joints and partings in the layered andesite during wave impact. The subsequent transport of boulders to the proximal end of the spit was driven by vigorous storm-generated currents. Successive big storms may have moved the larger boulders piece-meal for shorter distances during each event. Over the 10,000-year span of the Holocene, 100 super-storms may have reached the upper Gulf of California. Such a reckoning is reasonable, given the spit's geometry and various internal boundaries demarcated by amalgamated bars (Figure 12). An episodic growth rate between 7 and 8 m/century is informed by the total length of the various components adding up to a composite total of 750 m. Whereas each cobble and boulder in the construction is ultimately traced to the sea cliffs on the island's north shore, the residency time of large blocks resting offshore also must be considered. Thus, large andesite blocks of considerable weight may sit offshore near the distal end of the spit for some time during which biological encrustations accumulate (Figure 11), before the block is shifted from inter-tidal waters up onto the spit during a major storm.

5.2. Inference from Historical Hurricanes

Hurricane Odile entered the Gulf of California as a Category 4 storm in September 2014 and its economic impact is regarded as one of the most destructive events to affect the peninsular state of Baja California Sur, having caused more than 1654 million USD in damage to coastal infrastructure largely as a result of high winds [1]. According to a subsequent assessment by Gross and Magar (2020) [3], the same storm had the capacity to damage tidal-energy transformers due to wind-driven waves if such mechanisms were in place as part of the energy grid serving the state of Baja California at the far end of the gulf in the north. No such infrastructure presently exists in the region, but the study offers a cautionary warning about the potential for such damage even in the upper part of the gulf where hurricanes typically degrade to tropical storms. The last major storm to have crossed the upper gulf was Hurricane Kathleen in September 1976 as a Category 3 hurricane [21]. The passage of time since that event is considerable in terms of human memory and may be thought of as a once in a lifetime event by local residents living around Bahía San Luis Gonzaga.

The peninsular region of western Mexico was spared a potentially catastrophic event during the 2015 storm season, when Hurricane Patricia formed as a Category 5 storm with wind speeds up to 346 km/h off the Mexican mainland well south of the Baja California peninsula. That storm still holds the record as the most powerful hurricane to have originated in the eastern North Pacific Ocean [24]. Only the storm's outer most bands brushed across the opening to the Gulf of California, but the center of the storm made landfall on the Mexican mainland after an unexpected turn to the east. Had Hurricane Patricia tracked into the Gulf of California, it was certain to have caused more damage to coastal infrastructure than Hurricane Odile during the previous season. The occurrence of these two powerful storms, one after the other in subsequent years, raises the question of accountability for storms attributed to 100-year events. With growing conditions of global warming now experienced

around the world, the increase of such events is sure to be compressed in frequency as suggested by re-evaluations of storm data on a decadal basis [25]. Under such circumstances, the study of coastal boulder deposits and their development in recent geologic time offers a window on natural processes of interest not only to geomorphologists but also to engineers challenged to design infrastructures better suited to withstand more intense storms and any future rise in sea level.

5.3. Comparison with Other Gulf of California Deposits

Study of coastal boulder deposits (CBDs) and related boulder barrier deposits (BBDs) in the Gulf of California is a pursuit that has gained momentum during the last few years but, heretofore, only in the lower Gulf of California [9–11]. This contribution is the first to focus on the upper Gulf of California, a region generally thought to be impacted much less from the severity of hurricanes than the more southern parts closer to the Tropic of Cancer. Earlier work looked at limestone boulders pulled by storm action from Pliocene sea cliffs on Isla del Carmen, where a line of eroded boulders sits high on a marine terrace [9]. In this regard, the Carmen example conforms to a classic CBD pealed back from the front of a sea cliff by storm-related overwash. The Isla San Luis Gonzaga example in this study corresponds to the formation of boulder bars, where large blocks of andesite are leveraged from joint-bound layers at the base of sea cliffs and transported laterally by storm-generated currents where they accumulate as spits. Compared to previous examples in the southern Gulf region also formed by volcanic boulders derived from joint-bound blocks [11,12], the Isla San Luis Gonzaga structure is larger and more complex with components that can be differentiated as having accumulated during discrete storm events. For example, the earliest phases of extension ending beyond transect 3 off Isla San Luis Gonzaga (Figure 12a) are comparable to the half-ring structure constructed from rhyolite boulders at Ensenada Almeja [10]. The Almeja structure traces a pattern of clockwise extension stretching in an arc over a distance of about 250 m from the original bedrock source with joint-bound blocks. That pattern is replicated in the same dimensions by the earliest phases of construction at Isla San Luis Gonzaga. In both examples, fewer boulders are found on top of the bar closer to its termination, suggesting that wave energy declined with distance from the proximal end of those structures at the bedrock source.

After isolation of the spur leading to transect 3 from the rest of the spit at Isla San Luis Gonzaga (Figure 12b), new growth was extended in a strictly linear fashion similar to the unidirectional extension of bars across the front of Puerto Escondido in the lower Gulf of California [11]. There, two bars follow a linear fault trace with a small island connected in between. Not including the islet, the two bars extend for a length of 250 and 140 m, respectively. By comparison, the apparent length of the Gonzaga spit amounts to 450 m. However, development of parallel bars that became progressively attached to the core from one side, the total length of component parts including duplications amounts to a distance of 750 m. As such, the Gonzaga spit is one of most complex structures of its kind formed by loose cobbles and boulders in the entire Gulf of California region. Based on shape analyses from the various localities throughout the gulf region, there is little difference in the blocks of rock that were worn by marine erosion from limestone, rhyolite, and andesite into oblong cobbles and boulders. The factor that makes results of the Isla San Luis Gonzaga study so important is the apparent correspondence between extraordinary size, complexity, and the length of time necessary for development of BBDs. Given the weight of the largest boulders distributed across much of the Isla San Luis Gonzaga spit, it is apparent that their transport occurred during episodic hurricanes of high intensity. With greater attention to examples of CBDs throughout the Gulf of California and the expectation that the frequency of future hurricanes is likely to increase, it is proposed that known sites [9–11] including the Isla San Luis Gonzaga spit be monitored for changes once a selection of the largest boulders is tagged for reference.

5.4. Comparison with island deposits in the North Atlantic

Studies on CBDs on islands in the North Atlantic Ocean show much promise for similar research applying the same kind of analyses performed in the Gulf of California. An identical program using the same techniques of analyses for boulder shapes and sizes was conducted on modern and Pleistocene

CBDs on Santa Maria Island in the Azores [26]. In particular, the same equations have been applied to estimate wave heights during the Late Pleistocene (Marine Isotope Substage 5e) on basalt-dominated shores dated by fossils to approximately 125,000 years ago. Future studies that incorporate Pleistocene fossils may be expected in other Atlantic archipelagos such as the Canary and Cape Verde Islands.

6. Conclusions

Satellite tracking for hurricanes and typhoons has improved the ability of meteorologists to gather and analyze data on changes in atmospheric pressure, wind speed, and other factors that make statistical predictions based on recurrent circulation patterns increasingly accurate on a global basis [24]. Historically, few of the big storms generated in the NE Pacific Ocean actually deviate in direction to enter Mexico's Gulf of California from their point of origin farther south off the western mainland [1]. Those that do are generally found to rapidly deteriorate from hurricane strength to that of lesser tropical storms [21]. In contrast, the recent geologic record from the Holocene expands the time frame for evaluation of storms equilibrated with deposits of eroded shoreline materials and their bearing on coastal geomorphology. The present study on the complex boulder bar associated with Isla San Luis Gonzaga in the upper Gulf of California permits the following conclusions:

(1) Coastal boulder deposits and related boulder bars are described from the lower Gulf of California that experience episodic hurricanes, but the Isla San Luis Gonzaga spit composed of unconsolidated materials in the upper Gulf of California is larger and more complex than any features previously studied in the Lower Gulf of California.

(2) All cobbles and boulders entrained in the 450-m long structure are derived from andesite sea cliffs with joint-bound blocks on the north side of Isla San Luis Gonzaga, bypassing a well-defined marine terrace from the Late Pleistocene.

(3) Extensive data on variations in shape collected from seven transects across the structure show that clasts are mostly elongated in configuration. Data on variations in clast size from the same transects indicate changing ratios between boulders and cobbles that fall from 3:1 in favor of boulders to more equitable proportions in a progression toward the end of the structure.

(4) Despite a general decrease in the boulder population along the length of the structure, large boulders continue to be present even in the most distal parts of the structure and the estimated wave heights required to move those blocks into place entails an average height of 5 m.

(5) The overall complexity of the structure includes parallel bars that form side-by side as distinct swales through the distal half of the spit. These are interpreted as discrete additions from episodic storms. Assuming the structure began to form at the start of the Holocene, there was sufficient time for multiple mega-storms to reach the upper Gulf of California at a general rate of one per century to yield a possible growth rate between 7 and 8 m/century.

(6) Civil engineers evaluate hurricane damage to infrastructure as due to storm wind speed ashore and the impact of wave surge in coastal waters, but the geomorphology of coastal boulder deposits and related boulder bars provides another means to assess the potential for storm risk in regions like Mexico's Baja California peninsula and the adjacent Gulf of California.

(7) The concept of the 100-year storm as an event exceeding human memory at any point in time has changed during the historic rise in global warning experienced over the last two decades. It is not a question of if, but rather when, the next hurricane comparable to the Category 5 Patricia in 2014 will strike the gulf coast of Mexico's Baja California peninsula. As a follow-up to the region's various studies on coastal boulder deposits, consideration must be given to a monitoring program whereby some of the largest boulders are tagged to test movements after the next big storm.

Author Contributions: Conceptualization, R.G.-F. and J.L.-V.; methodology, R.G.-F. and M.A.S.R.-d.R.; software and validation, Á.R.H.-G.; formal analysis, writing, and draft preparation, M.E.J. All authors have read and agreed to the published version of the manuscript.

Funding: We are grateful to the Universidad Autónoma de Baja California for its support in collecting and processing the baseline information reported, herein, as part of the research project "Campaña Exploratoria para Inventariar el Patrimonio Geológico del Corredor Turístico Pluertecitos—San Luis Gonzaga Ensenada B.C., México" Programmatic number 388, supported in the *20va Convocatoria de Apoyo a Proyectos de Investigación*.

Acknowledgments: The following faculty and students from the Univesidad Autónoma de Baja California are thanked for their participation during field work on Isla San Luis Gonzaga: Miguel Agustín Téllez-Duarte, Cesar Omar Luna-Miyaki, and Josseline Michelle Crus-Pérez. Five readers contributed peer reviews with useful comments that led to the improvement of this contribution. Application of the equations used in this study is the sole responsibility of the authors.

Conflicts of Interest: The authors declare no conflicts of interest.

Appendix A

Table A1. Quantification of boulder size, volume, and estimated weight from selected coastal bar samples through transect 1 at Bahía San Luis Gonzaga. EWH = estimated wave height. The density of Baja Californian andesite at 2.3 gm/cm^2 is applied uniformly in order to calculate wave height for each boulder.

Sample	Long Axis (cm)	Intermediate Axis (cm)	Short Axis (cm)	Volume (cm^3)	Adjust to 75%	Weight (kg)	EWH Nott [18] (m)	EWH Pepe [20] (m)
1	80	55	50	220,000	165,000	421	5.6	8.0
4	42	28	13	15,288	11,466	29	3.0	2.1
6	68	60	53	216,240	162,180	414	4.8	8.4
8	32	22	10	7040	5280	13	2.3	1.6
10	38	27	16	16,416	12,312	31	2.7	2.5
12	50	29	10	14,500	10,875	28	3.5	1.6
14	46	30	12	16,560	12,420	32	3.2	1.9
16	40	28	11	12,320	9240	24	2.8	1.8
19	50	28	25	35,000	26,250	67	3.5	4.0
21	60	45	21	56,700	42,525	108	4.2	3.3
23	90	76	48	328,320	246,240	628	6.3	7.6
27	56	40	12	26,880	20,160	51	3.9	1.9
29	44	30	15	19,800	14,850	38	3.1	2.4
31	57	29	17	28,101	21,076	54	4.0	2.7
35	25	13	7	2275	1706	4.4	1.8	1.1
37	27	22	11	6534	4900	12.5	1.9	1.8
40	53	48	15	38,160	28,620	73	3.7	2.4
42	28	23	15	9660	7245	18.5	2.0	2.4
44	40	24	20	19,200	14,400	37	2.8	3.2
46	27	21	20	11,340	8505	22	1.9	3.2
49	32	30	24	23,040	17,280	44	2.3	3.8
52	35	28	20	19,600	14,700	37	2.5	3.2
56	50	20	18	18,000	13,500	34	3.5	2.9
59	59	30	23	40,710	30,533	78	4.2	3.7
63	28	21	20	11,760	8,820	22.5	2.0	3.2
65	46	40	37	68,080	51,060	130	3.2	5.9
70	30	23	16	11,040	8280	21	2.1	2.5
73	44	35	16	24,640	18,480	47	3.1	2.5
77	27	22	10	5940	4455	11.4	1.9	1.6
80	41	35	22	31,570	23,678	60	2.9	3.5
82	25	16	10	4000	3000	7.5	1.8	1.6
87	25	14	4	1400	1050	2.8	1.8	0.6
Mean	43.6	31	19	42,504	31,878	81	3.1	3.1

Table A2. Quantification of boulder size, volume, and estimated weight from selected coastal bar samples through transect 2 at Bahía San Luis Gonzaga. EWH = estimated wave height. The density of Baja Californian andesite at 2.3 gm/cm^2 is applied uniformly in order to calculate wave height for each boulder.

Sample	Long Axis (cm)	Intermediate Axis (cm)	Short Axis (cm)	Volume (cm^3)	Adjust to 75%	Weight (kg)	EWH Nott [18] (m)	EWH Pepe [20] (m)
1	33	25	24	19,800	14,850	38	2.3	3.8
5	47	35	33	54,285	40,714	104	3.3	5.3
7	42	22	20	18,480	13,860	35	3.0	3.2
9	52	40	35	72,800	54,600	139	3.7	5.6
11	58	47	26	70,876	53,157	136	4.1	4.1
13	31	18	6	3348	2511	6.4	2.2	1.0
15	50	29	16	23,200	17,400	44	3.5	2.5
17	36	13	11	5148	3861	9.8	2.5	1.8
20	54	37	25	49,550	37,463	96	3.8	4.0
22	46	25	18	20,700	15,525	40	3.2	2.9
23	42	33	18	328,320	246,240	628	3.0	2.9
26	28	21	10	5880	4410	11	2.0	1.6
28	26	24	10	6240	4680	12	1.8	1.6
30	33	30	29	28,710	21,533	55	2.3	4.6
32	28	18	12	6048	4536	12	2.0	1.9
34	30	15	7	3150	2363	6	2.1	1.1
39	29	23	11	7337	5503	14	2.0	1.8
41	45	25	24	27,000	20,250	52	3.2	3.8
45	39	36	18	25,272	18,954	48	2.7	2.9
47	50	38	16	30,400	22,800	58	3.5	2.5
51	44	20	12	10,560	7,920	20	3.1	1.9
53	64	51	11	35,904	26,928	69	4.5	1.8
55	30	30	18	16,200	12,150	31	2.1	2.9
57	50	28	8	11,200	8400	21	3.5	1.3
59	44	42	10	18,480	13,860	35	3.1	1.6
63	43	23	13	12,857	9643	25	3.0	2.1
66	29	28	20	16,240	12,180	31	2.0	3.2
68	41	36	13	19,188	14,391	37	2.9	2.1
73	37	29	20	21,460	16,095	41	2.6	3.2
75	26	19	15	7410	5558	14	1.8	2.4
77	40	25	25	25,000	18,750	48	2.8	4.0
80	23	23	8	4600	3450	8.8	1.6	1.3
84	36	21	18	13,608	10,206	26	2.5	2.9
Mean	40	28	17	30,886	23,174	59	2.8	2.7

Table A3. Quantification of boulder size, volume, and estimated weight from selected coastal bar samples through transect 3 at Bahía San Luis Gonzaga. EWH = estimated wave height. The density of Baja Californian andesite at 2.3 gm/cm^2 is applied uniformly in order to calculate wave height for each boulder.

Sample	Long Axis (cm)	Intermediate Axis (cm)	Short Axis (cm)	Volume (cm^3)	Adjust to 75%	Weight (kg)	EWH Nott [18] (m)	EWH Pepe [20] (m)
1	31	16	6	2976	2232	5.7	2.2	1.0
17	61	38	8	18,544	13,908	35	4.3	1.3
19	31	14	9	3906	2930	7.5	2.2	1.4
40	40	27	8	8640	6480	16.5	2.8	1.3
76	28	14	8.5	3332	2499	6.4	2.0	1.4
77	31	13	7	2821	2116	5.4	2.2	1.1
Mean	36	20.3	7.75	5664	4248	12.75	2.6	1.2

Table A4. Quantification of boulder size, volume, and estimated weight from all coastal bar boulders through transect 4 at Bahía San Luis Gonzaga. EWH = estimated wave height. The density of Baja Californian andesite at 2.3 gm/cm^2 is applied uniformly in order to calculate wave height for each boulder.

Sample	Long Axis (cm)	Intermediate Axis (cm)	Short Axis (cm)	Volume (cm^3)	Adjust to 75%	Weight (kg)	EWH Nott [18] (m)	EWH Pepe [20] (m)
1	27	20	10	5400	4050	10	1.9	1.6
2	70	39	30	81,900	61,425	157	4.9	4.8
3	39	20	12	9360	7020	18	2.7	1.9
7	63	39	20	49,140	36,855	94	4.4	3.2
8	75	38	35	99,750	74,813	191	5.3	5.6
9	25	14	12	4200	3150	8	1.8	1.9
10	38	29	19	20,938	15,704	40	2.7	3.0
12	29	23	17	11,339	8504	22	2.0	2.7
13	43	27	19	22,059	16,544	42	3.0	3.0
14	42	26	16	17,472	13,104	33	3.0	2.5
15	28	11	7	2156	1617	4	2.0	1.1
16	28	20	8	4480	3360	8.6	2.0	1.3
17	29	20	10	5800	4350	11	2.0	1.6
18	48	25	20	24,000	18,000	46	3.4	3.2
19	63	27	23	39,123	29,342	75	4.4	3.7
20	27	14	13	4914	3686	9	1.9	2.1
22	44	25	10	11,000	8250	21	3.1	1.6
25	40	34	15	20,400	15,300	39	2.8	2.4
26	32	23	5	3680	2760	7	2.3	0.8
27	61	25	19	28,975	21,731	55	4.3	3.0
29	38	27	13	13,338	10,004	26	2.7	2.1
31	40	16	15	9600	7200	18	2.8	2.4
32	50	34	25	42,500	31,875	81	3.5	4.0
34	35	19	18	11,970	8978	23	2.5	2.9
35	35	23	10	8050	6038	15	2.5	1.6
36	33	24	10	7920	5940	15	2.3	1.6
37	28	13	20	7280	5460	14	2.0	3.2
40	27	20	11	5940	4455	11	1.9	1.8
41	30	21	10	6300	4725	12	2.1	1.6
42	40	20	13	10,400	7800	20	2.8	2.1
45	40	38	10	15,200	11,400	29	2.8	1.6
48	27	17	10	4590	3443	9	1.9	1.6
Mean	40	24	15	19,037	14,278	36	2.8	2.4

Table A5. Quantification of boulder size, volume, and estimated weight from all coastal bar boulder through transect 5 at Bahía San Luis Gonzaga. The density of Baja Californian andesite at 2.3 gm/cm^2 is applied uniformly in order to calculate wave height for each boulder.

Sample	Long Axis (cm)	Intermediate Axis (cm)	Short Axis (cm)	Volume (cm^3)	Adjust to 75%	Weight (kg)	EWH Nott [18] (m)	EWH Pepe [20] (m)
1	57	40	38	86,640	64,980	166	4.0	6.1
2	38	26	9	8892	6669	17	2.7	1.4
3	35	32	4	4480	3360	8.6	2.5	0.6
7	40	23	10	9200	6900	17.6	2.8	1.6
8	27	20	9	4860	3645	9.3	1.9	1.4
10	32	23	10	7360	5520	14	2.3	1.6
18	26	24	14	8736	6552	17	1.8	2.2
19	25	12	10	3000	2250	5.7	1.8	1.6
20	36	27	14	13,608	10,206	26	2.5	2.2

Table A5. *Cont.*

Sample	Long Axis (cm)	Intermediate Axis (cm)	Short Axis (cm)	Volume (cm^3)	Adjust to 75%	Weight (kg)	EWH Nott [18] (m)	EWH Pepe [20] (m)
24	35	23	12	9660	7245	18.5	2.5	1.9
29	55	31	25	42,625	31,969	82	3.9	4.0
30	44	40	23	4480	3360	8.6	3.1	3.7
33	37	33	26	31,746	23,910	61	2.6	4.1
37	25	18	17	7650	5738	14.6	1.8	2.7
38	38	23	8	6992	5244	13	2.7	1.3
44	30	19	12	6840	5130	13	2.1	1.9
46	79	43	21	71,337	53,503	136	5.6	3.3
47	35	17	12	7140	5355	14	2.5	1.9
56	36	20	12	8640	6480	17	2.5	1.9
101	42.5	28	19	22,610	16,958	43	3.0	3.0
102	39	23	13	11,661	8746	22	2.7	2.1
103	42	24	6	6048	4536	11.5	3.0	1.0
104	26	21	10	5460	4095	10	1.8	1.6
106	36	25	11	9900	7425	19	2.5	1.8
107	45	18	14	11,340	8505	22	3.2	2.2
108	34	24	7	5712	4284	11	2.4	1.1
115	28	26	12	8736	6552	17	2.0	1.9
119	40	30	12	14,400	10,800	27.5	2.8	1.9
123	25	15	15	5625	4219	11	1.8	2.4
Mean	37.5	25	14	15,358	11,519	29.4	2.6	2.2

Table A6. Quantification of boulder size, volume, and estimated weight from all coastal bar boulders through transect 6 at Bahía San Luis Gonzaga. EWH = estimated wave height. The density of Baja Californian andesite at 2.3 gm/cm^2 is applied uniformly in order to calculate wave height for each boulder.

Sample	Long Axis (cm)	Intermediate Axis (cm)	Short Axis (cm)	Volume (cm^3)	Adjust to 75%	Weight (kg)	EWH Nott [18] (m)	EWH Pepe [20] (m)
1	33	22	22	15,972	11,979	30.5	2.3	3.5
2	37	30	12	13,320	9990	17	2.6	1.9
3	39	33	5	6435	4826	8.6	2.7	0.8
15	40	23	14	12,880	9660	24.6	2.8	2.2
16	39	30	25	29,250	21,938	56	2.7	4.0
20	29	26	6	4524	3393	8.6	2.0	1.0
26	29	19	11	6061	4546	12	2.0	1.8
30	80	54	23	99,360	74,520	190	5.6	3.7
41	26	21	6	3276	2457	6	1.8	1.0
69	31	26	7	5642	4232	11	2.2	1.1
73	44	16	14	9856	7392	19	3.1	2.2
80	27	14	8	3024	2268	6	1.9	1.3
83	26	18	13	6084	4563	12	1.8	2.1
93	35	15	7	3675	2756	7	2.5	1.1
94	32	24	23	17,664	13,248	34	2.3	3.7
96	37	25	11	10,175	7631	20	2.6	1.8
97	26	16	13	5408	4056	10	1.8	2.1
101	38	16	12	7296	5472	14	2.7	1.9
102	26	13	11	3718	2789	7	1.8	1.8
103	34	19	9	5814	4361	11	2.4	1.4
Average	35	23	12.6	13,472	10,104	25	2.5	2.0

Table A7. Quantification of boulder size, volume, and estimated weight from selected coastal bar samples through transect 7 at Bahía San Luis Gonzaga. EWH = estimated wave height. The density of Baja Californian andesite at 2.3 gm/cm^2 is applied uniformly in order to calculate wave height for each boulder.

Sample	Long Axis (cm)	Intermediate Axis (cm)	Short Axis (cm)	Volume (cm^3)	Adjust to 75%	Weight (kg)	EWH Nott [18] (m)	EWH Pepe [20] (m)
5	53	49	32	83,104	62,328	159	3.7	5.1
7	58	41	20	47,560	35,670	91	4.1	3.2
12	26	15	12	5760	4320	11	1.8	1.9
15	34	22	15	11,220	8415	22	2.4	2.4
17	38	26	15	14,820	11,115	28	2.7	2.4
21	55.5	53	41	120,602	90,451	231	3.9	6.5
24	44	25	22	24,200	18,150	46	3.1	3.5
29	30	29	24	20,880	15,660	40	2.1	3.8
31	36	20	20	14,400	10,800	28	2.5	3.2
34	39	27	22	23,166	17,375	44	2.7	3.5
37	34	30	14	14,280	10,710	27	2.4	2.2
41	28	15	10	4200	3150	8	2.0	1.6
47	27	23	19	11,799	8849	23	1.9	3.0
50	44	20	14	12,320	9240	24	3.1	2.2
55	50	48	35	84,000	63,000	161	3.5	5.6
64	29	25	24	17,400	13,050	33	2.0	3.8
67	27	24	5	3240	2430	6	1.9	0.8
71	30	27	14	11,340	8505	22	2.1	2.2
73	26	22	14	8008	6006	15	1.8	2.2
79	25	16	12	4800	3600	9	1.8	1.9
81	52	29	13	19,604	14,703	38	3.7	2.1
83	27.5	19	12	6270	4703	12	1.9	1.9
88	30	26	14	10,920	8190	21	2.1	2.2
94	43	43	25	46,225	34,669	88	3.0	4.0
97	44	30	20	26,400	19,800	51	3.1	3.2
100	30	21	13	8190	6143	16	2.1	2.1
103	35	20	10	7000	5250	13	2.5	1.6
105	26	23	16	9568	7176	18	1.8	2.5
107	84	38	20	63,840	47,880	122	5.9	3.2
112	34	17	15	8670	6503	17	2.4	2.4
Mean	38	27	18	24,793	18,595	47	2.7	2.9

References

1. Romero-Vadillo, E.; Zaystev, O.; Morales-Pérez, R. Tropical cyclone statistics in the northeastern Pacific. *Atmósfera* **2007**, *20*, 197–213.
2. Muriá-Vila, D.; Jaimes, M.Á.; Pozos-Estrada, A.; López, A.; Reinoso, E.; Chávez, M.M.; Peña, F.; Sánchez-Sesma, J.; López, O. Effects of hurricane Odile on the infrastructure of Baja California Sur, Mexico. *Nat. Hazards* **2018**, *9*, 963–981. [CrossRef]
3. Gross, M.; Magar, V. Wind-induced currents in the Gulf of California from extreme events and their impact on tidal energy devices. *J. Mar. Sci. Eng.* **2020**, *8*, 80. [CrossRef]
4. Merrifield, M.A.; Winant, C.D. Shelf-circulation in the Gulf of California: A description of the variability. *J. Geophys. Res.* **1989**, *94*, 133–160. [CrossRef]
5. May, S.M.; Engel, M.; Brill, D.; Squire, P.; Scheffers, A.; Kelletat, D. Coastal hazards from tropical cyclones and extratropical winter storms based on Holocene storm chronologies. In *Coastal Hazards*; Finkl, C.W., Ed.; Coastal Research Library: Cham, Switzerland, 2013; Volume 6, pp. 557–585.
6. Switzer, A.D.; Burston, J.M. Competing mechanisms for boulder deposition on the southeast Australian coast. *Geomorpholgy* **2010**, *114*, 42–54. [CrossRef]

7. Buchanan, D.H.; Naylor, L.A.; Hurst, M.D.; Stephenson, W.J. Erosion of rocky shore platforms by block detachment from layered stratigraphy. *Earth Surf. Process. Landf.* **2019**, *45*, 1028–1037. [CrossRef]
8. Suursaar, Ü; Alari, V.; Tõnisson, H. Multi-scale analysis of wave conditions and coastal changes in the northeastern Baltic Sea. *J. Coast. Res.* **2014**, *70*, 223–228. [CrossRef]
9. Johnson, M.E.; Ledesma-Vázquez, J.; Guardado-France, R. Coastal geomorphology of a Holocene hurricane deposit on a Pleistocene marine terrace from Isla Carmen (Baja California Sur, Mexico). *J. Mar. Sci. Eng.* **2018**, *6*, 108. [CrossRef]
10. Johnson, M.E.; Guardado-France, R.; Johnsob, E.M.; Ledesma-Vázquez, J. Geomorphology of a Holocene Hurricane deposit eroded from rhyolite sea cliffs on Ensenada Almeja (Baja California Sur, Mexico). *J. Mar. Sci. Eng.* **2019**, *7*, 193. [CrossRef]
11. Johnson, M.E.; Johnson, E.M.; Guardado-France, R.; Ledesma-Vázquews, J. Holocene hurricane deposits eroded as coastal barriers from andesite sea cliffs at Puerto Escondido (Baja California Sur, Mexico). *J. Mar. Sci. Eng.* **2020**, *8*, 75. [CrossRef]
12. Backus, D.H.; Johnson, M.E.; Ledesma-Vazquez, J. Peninsular and island rocky shores in the Gulf of California. In *Atlas of Coastal Ecosystems in the Western Gulf of California*; Johnson, M.E., Ledesma-Vazquez, J., Eds.; University Arizona Press: Tucson, AZ, USA, 2009; pp. 11–27. ISBN 978-0-8165-2530-0.
13. Gastil, R.G.; Phillips, R.P.; Allison, E.C. *Reconnaissance Geological Map of the State of Baja California*; Geological Society America; Map Sheets a, b, and c; Geological Society of America: Boulder, CO, USA, 1971.
14. Wentworth, C.K. A scale of grade and class terms for clastic sediments. *J. Geol.* **1922**, *27*, 377–392. [CrossRef]
15. Sneed, E.D.; Folk, R.L. Pebbles in the lower Colorado River of Texas: A study in particle morphogenesis. *J. Geol.* **1958**, *66*, 114–150. [CrossRef]
16. Yeh, F.-H.; Huang, C.-J.; Han, J.-Y.; Ge, L. Modeling slope topography using unmanned aerial vehicle image technique. *MATEC Web Conf.* **2018**, *147*, 07002. [CrossRef]
17. Casella, E.; Drechsel, J.; Winbter, C.; Benninghoff, M.; Rovere, A. Accuracy of sand beach topography surveying by drones and photogrammetry. *Geo-Mar. Lett.* **2020**, *40*, 255–268. [CrossRef]
18. Nott, J. Waves, coastal bolder deposits and the importance of pre-transport setting. *Earth Planet. Sci. Lett.* **2003**, *210*, 269–276. [CrossRef]
19. Nandasena, N.A.K.; Paris, R.; Tanaka, N. Reassessment of hydrodynamic equations: Minimum flow velocity to initiate boulder transport by high energy events (storms, tsunamis). *Mar. Geol.* **2011**, *281*, 70–84. [CrossRef]
20. Pepe, F.; Corradino, M.; Parrino, N.; Besio, G.; Presti, V.L.; Renda, P.; Calcagnile, L.; Quarta, G.; Sulli, A.; Antonioli, F. Boulder coastal deposits at Favignana Island rocky coast (Sicily, Italy): Litho-structural and hydrodynamic control. *Geomorphology* **2018**, *303*, 191–209. [CrossRef]
21. Rebman, J.P.; Roberts, N.C. *Baja California Plant Field Guide*, 3rd ed.; Sun Belt Publications: San Diego, CA, USA, 2012; p. 451. ISBN 978-0-916251-18-5.
22. Brusca, R.C. *Common Intertidal Invertebrates of the Gulf of California*, 2nd ed.; University of Arizona Press: Tucson, AZ, USA, 1980; p. 513. ISBN 0-8165-0682-5.
23. Nott, J.; Haig, J.; Neil, H.; Gillierson, D. Greater frequency of landfalling tropical cyclones at centennial compared to seasonal and decadal scales. *Earth Planet. Sci. Let.* **2007**, *255*, 367–372. [CrossRef]
24. Avila, L. The 2015 Eastern North Pacific Hurricane Season: A very active year. *Weatherwise* **2016**, *69*, 36–42. [CrossRef]
25. Kossin, J.P.; Knapp, K.R.; Olander, T.L.; Velden, C.S. Global increase in major tropical cyclone exceedance probability over the past four decades. *Proc. Natl. Acad. Sci. USA* **2020**, *117*, 11975–11980. [CrossRef]
26. Ávila, S.P.; Johnson, M.E.; Rebelo, A.C.; Baptista, L.; Melo, C.S. Comparison of modern and Pleistocene (MIS 5e) coastal Boulder deposits from Santa Maria Island (Azores Archipelago, NE Atlantic Ocean). *J. Mar. Sci. Eng.* **2020**, *8*, 386. [CrossRef]